Ain Shams Engineering Journal (2018) 9, 1439–1450

Ain Shams University

Ain Shams Engineering Journal

www.elsevier.com/locate/asej
www.sciencedirect.com

CIVIL ENGINEERING

Studying the effect of partial blockage on multi-vents bridge pier scour experimentally and numerically

Yasser Abdallah Mohamed Moussa [a,*], Tarek Hemdan Nasr-Allah [b], Amera Abd-Elhasseb [b]

[a] *Zagazig University, Faculty of Engineering, Egypt*
[b] *Benha University, Faculty of Engineering, Egypt*

Received 26 June 2016; revised 17 August 2016; accepted 6 September 2016
Available online 24 October 2016

KEYWORDS

Local scour;
Pier;
Abutment;
Blockage;
SSIIM;
Hydraulic structures

Abstract The local scour depth at bridge supports due to partial blockage on front of multi-vents bridge pier is studied experimentally and numerically. The existence of blockage such as debris and industrial wastes, leads to increase the local scour depth around bridge foundation and even bridge failure. The computational fluid dynamic program (SSIIM), is applied to simulate the scour around bridge supports. The numerical model used the finite-volume method to solve the Navier-Stokes equations. The k–ε turbulence model is applied to solve the Reynolds-stress term. The 3-D flow model has been verified by comparing the numerical simulation with experimental data. It was found that, the local scour depth by impermeable obstruction on front of one bridge pier depends on Froude number, and dimensions of obstacle. In addition, multiple linear repressions are used to propose empirical equations for estimating local scour depth at bridge supports. The results show good agreement between both of numerical and statistical simulations with experimental results.

1. Introduction

Bridge failures are caused by various reasons, but the main reason is caused by scour around bridge supports. Most of hydraulic structures such as bridges and culverts suffer from heavy infestation of floating as well as submerged debris that accumulates and obstructs its waterway entrance. The accumulation of debris around bridge supports or through bridge vents causes higher velocities and vortices resulting in larger dimensions for the induced scour. The basic mechanism causing local scour is the formation of vortices at their base. The supports of bridge (piers and abutments) objected the flow causing vortex, consequently the scour generated. The increase in the expected local scour depth owing to debris accumulation could be unsafe for bridge foundation [1]. Douglas and Smith [2] studied the effect of large debris on physical characteristics of sand-bed Rivers of the south-eastern USA. Bovis and Jakob

* Corresponding author.
E-mail address: Yasser_eng1997@zu.edu.eg (Y.A.M. Moussa).
Peer review under responsibility of Ain Shams University.

ELSEVIER Production and hosting by Elsevier

http://dx.doi.org/10.1016/j.asej.2016.09.010
2090-4479 © 2016 Ain Shams University. Production and hosting by Elsevier B.V.

Nomenclature

A_L	left abutment
Ar	right abutment
B_p	width of pier
C_b	concentration of sediment;
d	sediment particle diameter
D_{50}	median size of sand
d_s	maximum local scour depth
F_r	Froude number
g	gravitational acceleration
H	blockage height
K	Von Karmen constant
k_s	roughness height
L	blockage length
$\acute{L}$	length of bridge pier
P_L	left pier
Pr	right pier
q_b	bed load discharge
u	flow velocity
W	blockage width
y_t	tail water depth
τ	bed shear stress
τ_c	critical bed shear stress
ν	kinematic viscosity of the water
ρ_s	density of sediment
ρ_w	density of water

[3] applied statistical analysis to simulate large woody debris flow attributes. Pagliara and Carnacia [4] studied the effect of debris accumulation on scour formed at bridge foundation. Douglas et al. [5] clarified that, velocities are reduced by large woody debris in the bank toe zone. Bridge blockage, resulting from floating containers and woody debris, was studied [6–8]. Reynaud [9] developed the procedures for predicting the volume of debris accumulations at bridge supports and methods for estimating scour resulting from debris. The significant factors affecting the blocking probability at bridge foundation during flood events were evaluated by Schmocker and Hager [10]. The effect of blockage on scour formed upstream circular pier was studied by D'Alessandro [11]. Tejada [12] investigated the effect of blockage ratio and size of sediment materials on local scour depth around bridge pier. Maatooq [13] studied the effect of varying distances between pier and neighboring abutment on scour formation. Nasr-Allah et al. [14] investigated experimentally the effect of permeable obstruction on scour formed at bridge piers and abutments. Sanoussi and Habib [15] presented experimentally the local scour at rounded and sloped face piers with skew angles. Khwairakpam et al. [16] clarified the effect of varying water depths and densimetric Froude numbers on local scour depth at bridge pier. Local scour depth at bridge abutment provided with different shapes of collars was investigated experimentally and numerically by Mohamed et al. [17,18]. Nohani and Heidarnejad [19] studied experimentally the effect of flow angle of attack on local scour depth formed at slotted bridge pier. Akib et al. [20] clarified the relationship between local scour depth in complex pier groups and combined piles bridge for different flow velocities. Mohamed et al. [21] carried out an experimental study on scour characteristics formed around multi-vents bridge piers. It was concluded that using scour countermeasure such as collar, current deflectors, and sacrificial piles reduced the local scour depth by more than 87%. Nasr-Allah et al. [22] investigated scour formation at bridge supports experimentally and numerically. In the present paper, the effects of relative width and height of partial blockage at front of bridge pier on scour characteristics around the neighboring bridge supports were studied experimentally and numerically.

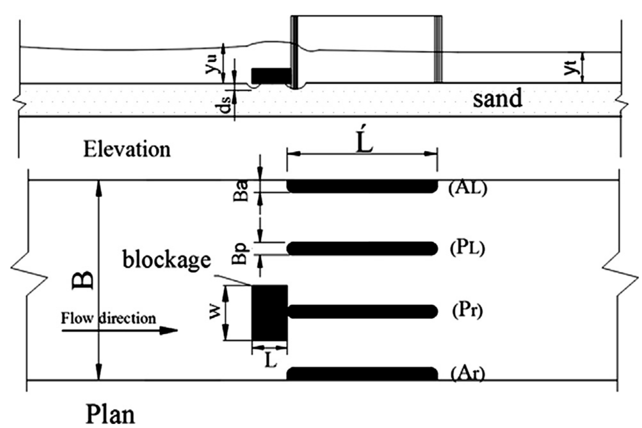

Figure 1 Definition sketch for experimental model.

Table 1 Arrangements debris height and width at nose of right pier.

Debris height (cm)	Debris width (cm)	Debris length (cm)	Width/Length	Height/pier width
1	5	7	0.7	0.4
1	5.9	5.9	1	0.4
1	7	5	1.4	0.4
1	8.75	4	2.2	0.4
1	11.7	3	4	0.4
1	17.5	2	8.75	0.4
2	6.2	2.8	2.2	0.8
3	5	2.3	2.2	1.2

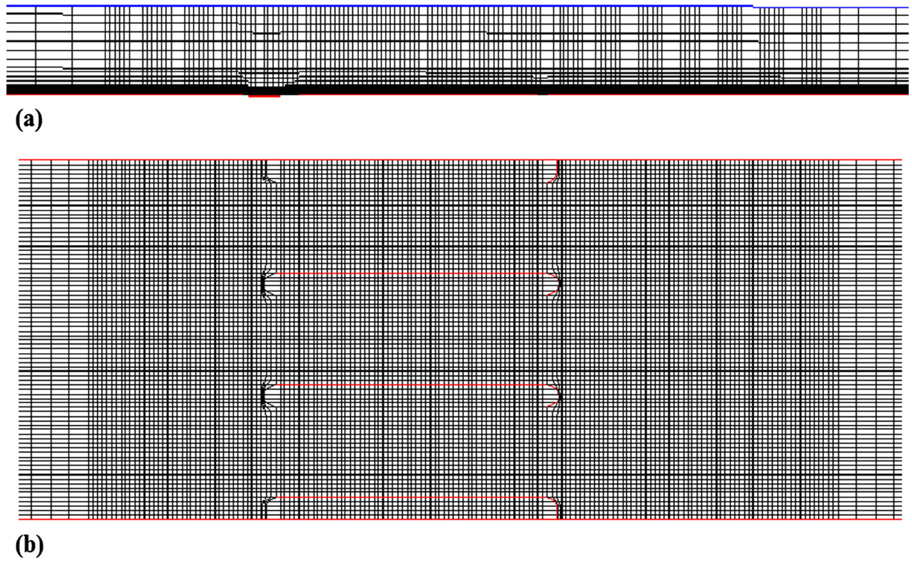

Figure 2 Grid information for (a) XZ-plane for computational grid. (b) XY-plane for computational grid.

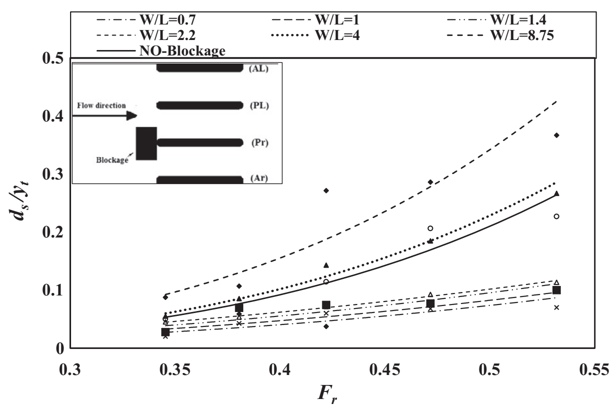

Figure 3 The relationship between d_s/y_t and F_r at blockage upstream right pier (Pr) for different ratios of W/L and $H/B_P = 0.4$.

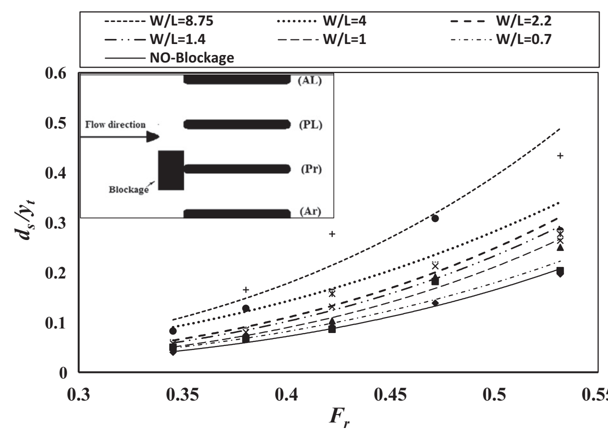

Figure 5 The relationship between d_s/y_t and F_r at right abutment (Ar) for different ratios of W/L and $H/B_P = 0.4$.

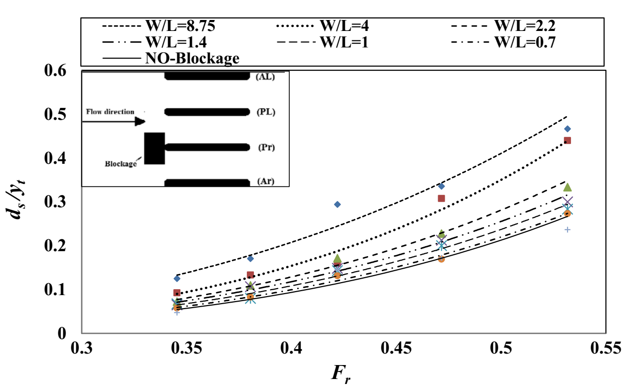

Figure 4 The relationship between d_s/y_t and F_r at left pier (P_L) for different ratios of W/L and $H/B_P = 0.4$.

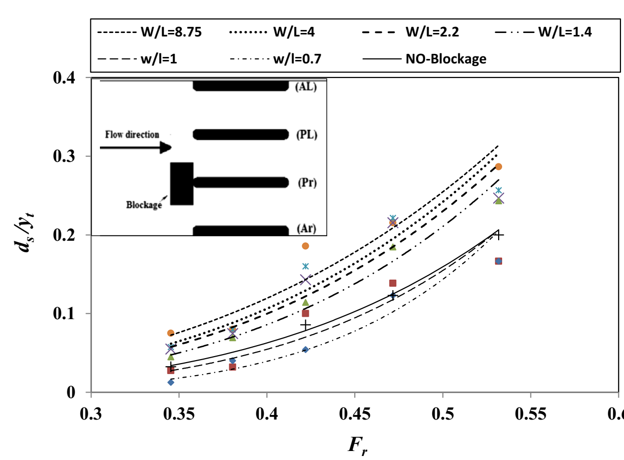

Figure 6 The relationship between d_s/y_t and F_r at left abutment (A_L) for different ratios of W/L and $H/B_P = 0.4$.

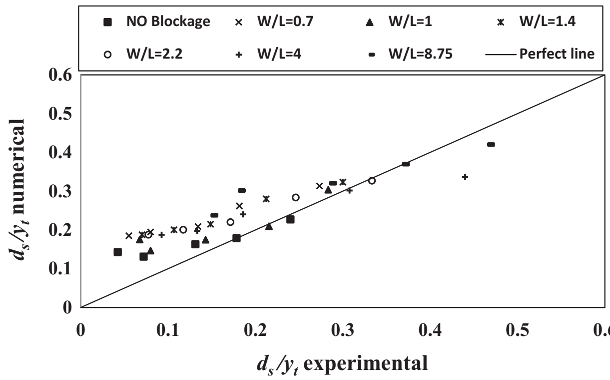

Figure 7 The numerical versus experimental results for different ratios of W/L.

2. Experimental work

The experimental work was carried out in a re-circulating open channel with dimensions of 0.4 m width, 0.20 m depth and length of 5.70 m. The rate of flow was measured using a pre-calibrated orifice meter fixed on the inlet feeding pipe. The tail gate was used to control water depth. The thickness of movable bed is 10 cm. The point gauge with accuracy of 0.1 mm was used to survey scour formed around bridge supports. Uniform grades of materials of mobile bed were used. The median size of sand (D_{50}) and geometric standard deviation were 0.75 mm and 1.27, respectively. The experimental work was conducted under clear-water scour condition. Two piers have circular shape at the nose and tail with 2.5 cm thickness and 40 cm length ($\acute{L}$). The width of each vent of bridge is 10 cm. The values of Froude numbers were ranging from 0.33 to 0.54. The time for each run was taken as 6 h at which more than 90% of the equilibrium scour was developed. The arrangements of impermeable blockage dimensions are shown in Table 1.

3. Dimensional analysis

The dimensional analysis was applied for correlating the variables affecting scour at bridge supports in the form of dimensionless groups, see Fig. 1. The scour depth ratio was correlated with the independent parameters as follows:

$$d_s/y_t = f(F_r, H/B_p, W/L) \tag{1}$$

in which d_s is the maximum scour depth; y_t is the tail water depth; F_r, is Froude number ($F_r = u/(gy_t)^{0.5}$, g is the gravitational acceleration, and u is the flow velocity); H is the blockage height; B_p is width of pier; L is blockage Length; and W is blockage width.

4. Numerical model

The computational fluid dynamic model SSIIM (Sediment Simulation In Intakes with Multiblock option) solves the equations of Navier-Stokes in three dimensional and general non-orthogonal. The control volume approach is applied to discretize Navier-Stokes equations. The Navier-Stokes equations for constant density and non-compressible have the following form:

$$\frac{\partial u_i}{\partial t} + \cup_j \frac{\partial u_i}{\partial x_j} = \frac{1}{\rho}\frac{\partial}{\partial x_j}\left[-\rho \overline{u_\imath}\,\overline{u_J} - p\delta_{ij}\right] \tag{2}$$

The transient is presented in the first term on the left hand side of Eq. (2). The convective term is next term. The first and second terms on the right side are the Reynolds stress and pressure terms, respectively. The k–ε turbulence model is used to estimate Reynolds-stress term. The rough boundaries on fluid dynamics are modeled using the wall law in SSIIM as follows:

$$\frac{U}{U_*} = \frac{1}{k}\ln(30z/k_s) \tag{3}$$

where k_s is the roughness height, K is Von Karman constant, U is the mean velocity, U_* is the shear velocity and z is the height above the bed. Fixed-lid approach is used to calculate free surface. SSIIM program uses Van Rijen's formula [23] to calculate the equilibrium sediment concentration close to the bed as follows:

$$C_b = 0.015\frac{d^{0.3}[(\tau-\tau_c)/\tau_c]^{0.5}}{z\left[\frac{(\rho_s-\rho_w)g}{\rho_w v^2}\right]} \tag{4}$$

where C_b is the concentration of sediment; d is the sediment particle diameter; z is a the height of roughness; τ is the bed shear stress, and τ_c is the critical bed shear stress; ρ_w and ρ_s are the density of water and sediment, respectively; ν is the kinematic viscosity of the water and g is the gravitational acceleration. Van Rijen's formula is used to compute the bed load discharge (q_b) [23] in the following form:

$$\frac{q_b}{D_{50}\sqrt[1.5]{((\rho_s-\rho_w)/\rho_w}} = 0.053\frac{d^{0.3}[(\tau-\tau_c)/\tau_c]^{0.5}}{D_{50}\sqrt[0.3]{\left[\frac{(\rho_s-\rho_w)g}{\rho_w v^2}\right]^{0.1}}} \tag{5}$$

where D_{50} is the mean size of sediment.

A structured grid mesh was generated, as shown in Fig. 2. A 3-D grid mesh was carried out with 234, 81 and 22 elements in the X, Y and Z directions, respectively. An uneven distribution of grid lines in both horizontal and vertical directions was used to get significant results in the area around bridge supports.

5. Analysis and discussion of results

5.1. Effects of different ratios of ($\mathbf{W}/\mathbf{L}$) on local scour depth

Local scour depth around multi-vents bridge pier as a result of impermeable obstruction at front of right pier (Pr) was investigated experimentally and numerically. Effect of different relative widths (W/L = 8.75, 4, 2.2, 1.4, 1.0, 0.71 and 0.11) of the obstacle on local scour depth around bridge supports was investigated at H/B_p = 0.4. The relationship between relative scour depth d_s/y_t and Froude number F_r upstream impermeable blockage at front of Pr is shown in Fig. 3. It was found that, the scour in front of the obstruction increases by increasing the ratios of W/L. For larger ratios of W/L (4.0 and 8.75), the local scour depth increased compared to the no-blockage case, due to the higher velocity concentration at the upstream face of the obstacle. This blockage represents a scour shelter to right pier (Pr) and on contrary it leads to increase the scour dimensions at the rest of the other bridge supports, see Figs. 4–6. The relationships between relative scour depth (d_s/y_t) and Froude number (F_r) for the left pier (P_L), right abutment (Ar) and left abutment (A_L) are shown in Figs. 4–6

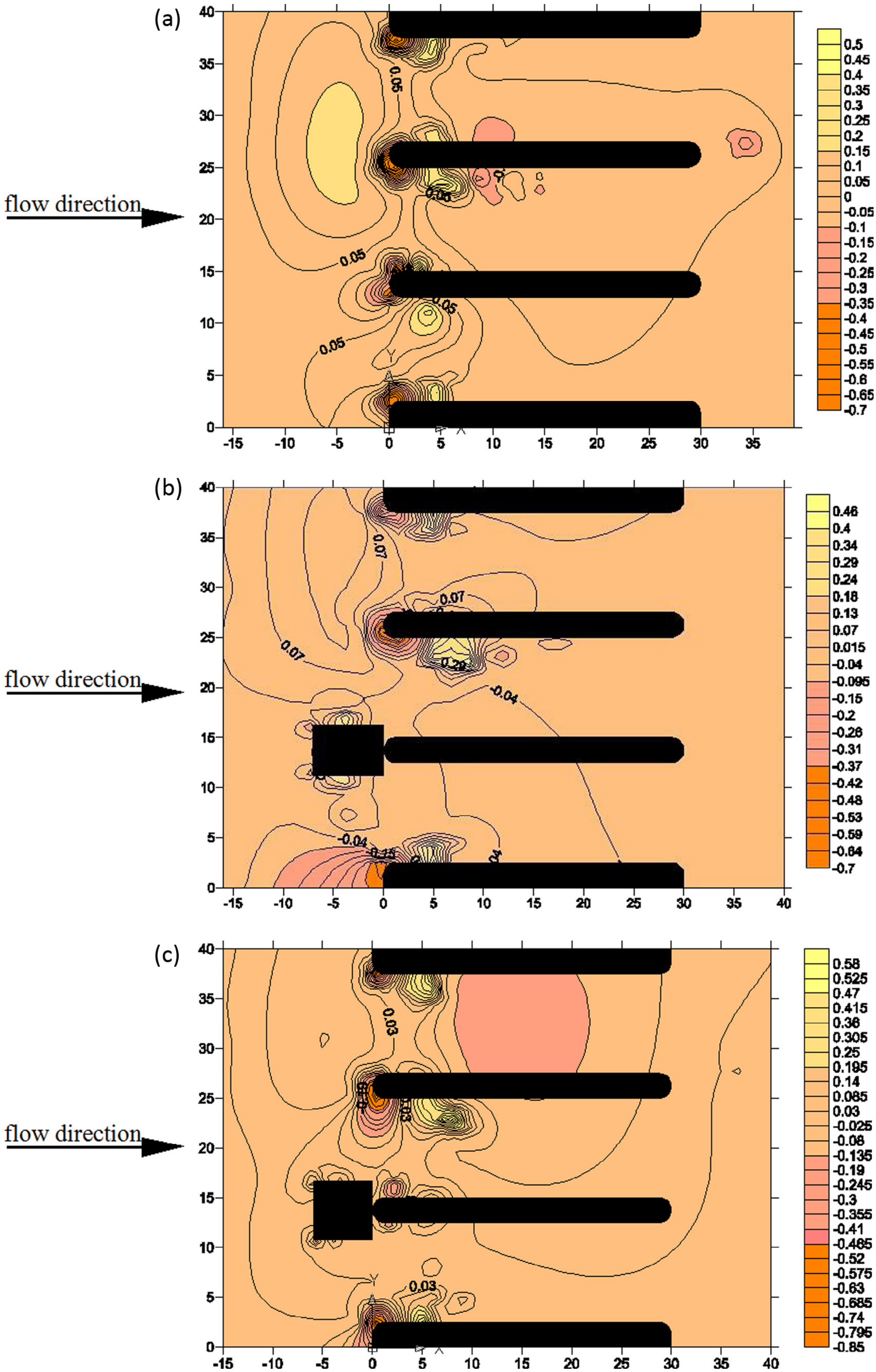

Figure 8 Scour contour maps for (a) No-Blockage, (b) $W/L = 0.7$, (c) $W/L = 1.0$, and (d), $W/L = 1.4$, (e) $W/L = 2.2$, (f) $W/L = 4.0$ and (g) $W/L = 8.75$ at $F_r = 0.53$ and $H/B_P = 0.4$.

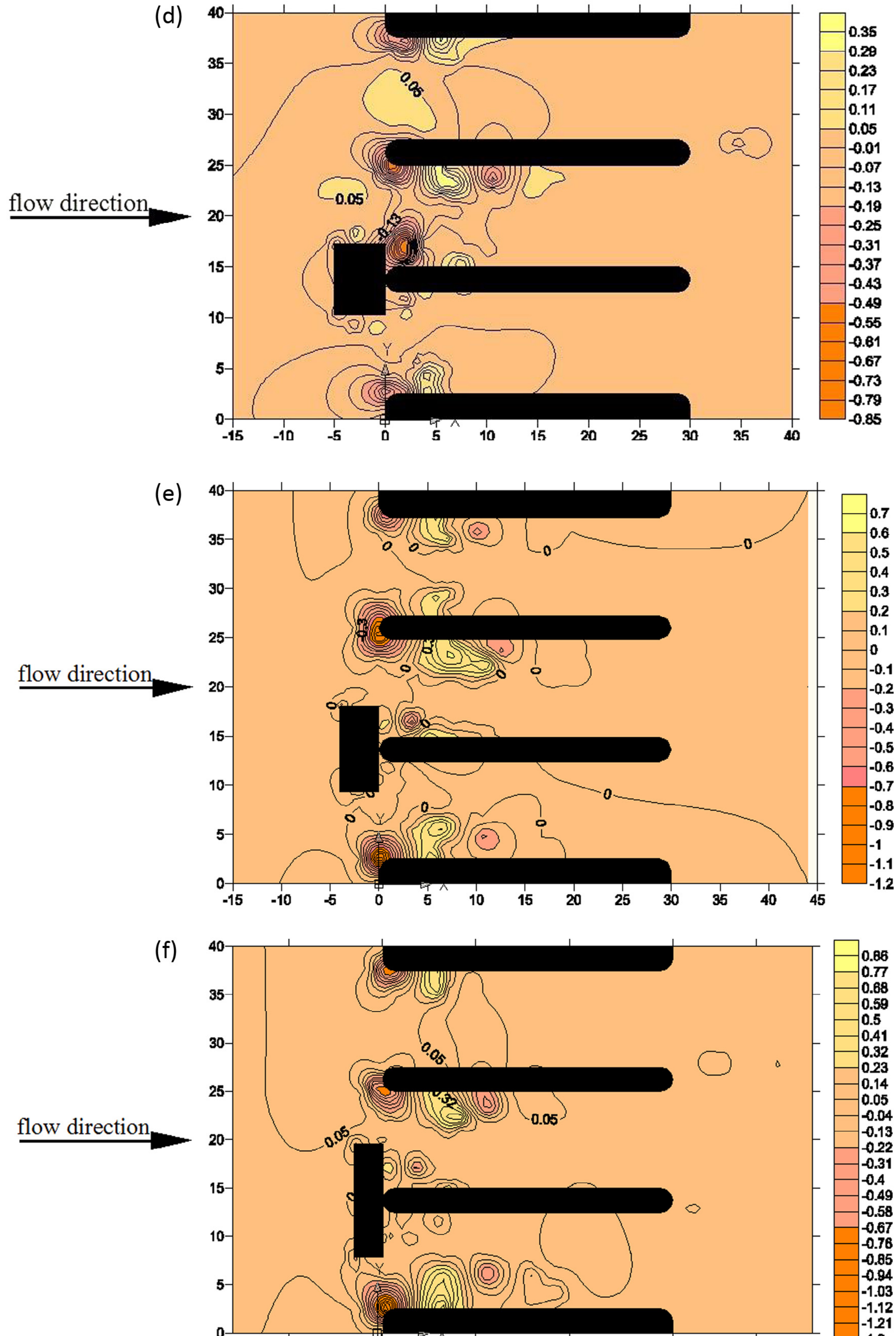

Fig. 8 (*continued*)

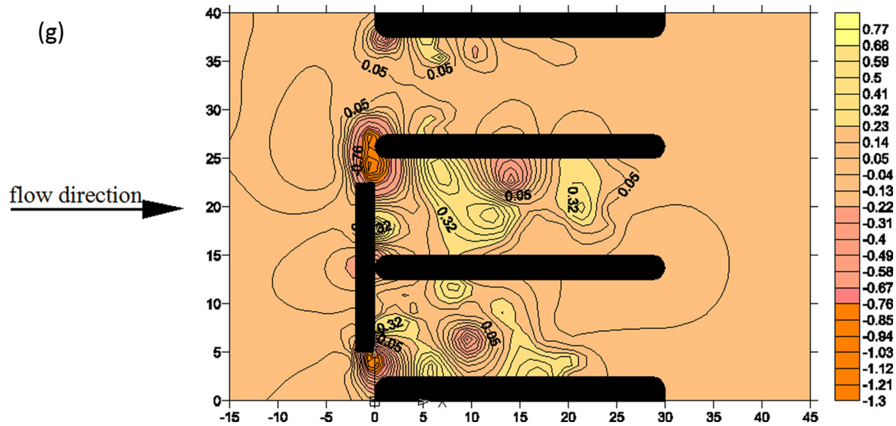

Fig. 8 (*continued*)

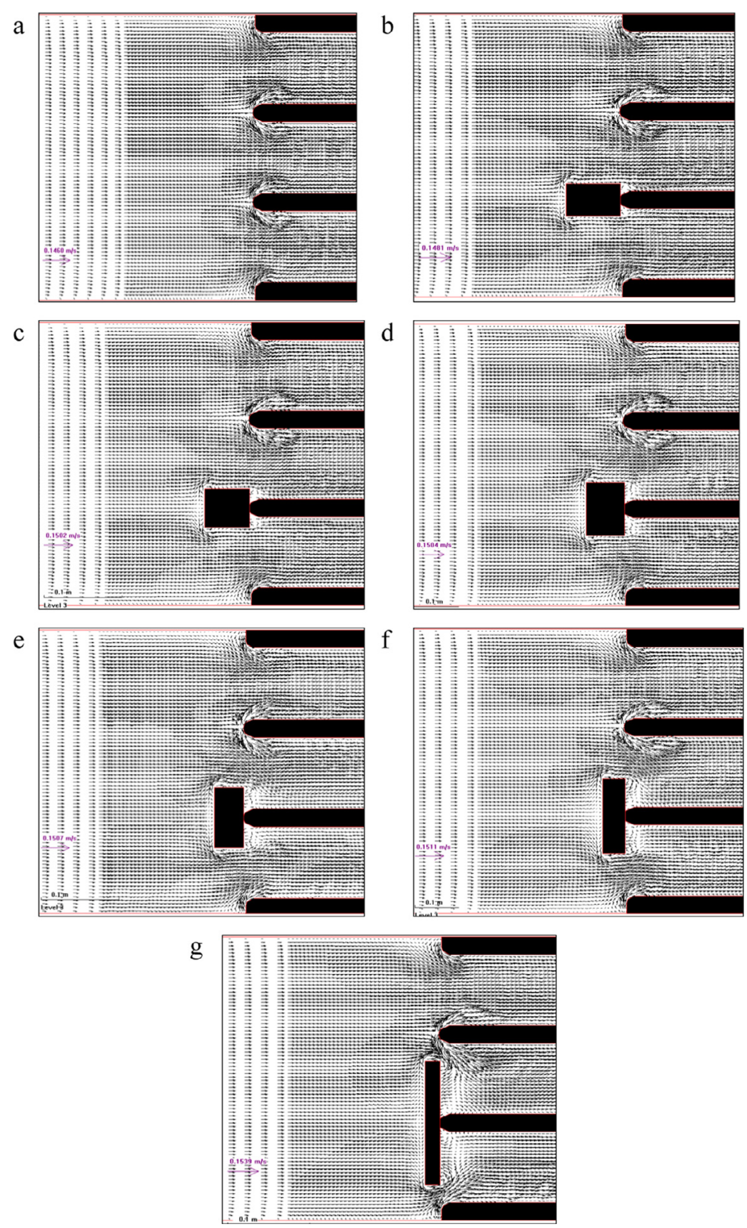

Figure 9 Horizontal distribution of velocity at distance 0.03 from water depth for (a) No-blockage, (b) $W/L = 0.7$, (c) $W/L = 1.0$, and (d), $W/L = 1.4$, (e) $W/L = 2.2$, (f) $W/L = 4.0$ and (g) $W/L = 8.75$ at $F_r = 0.53$ and $H/B_P = 0.4$.

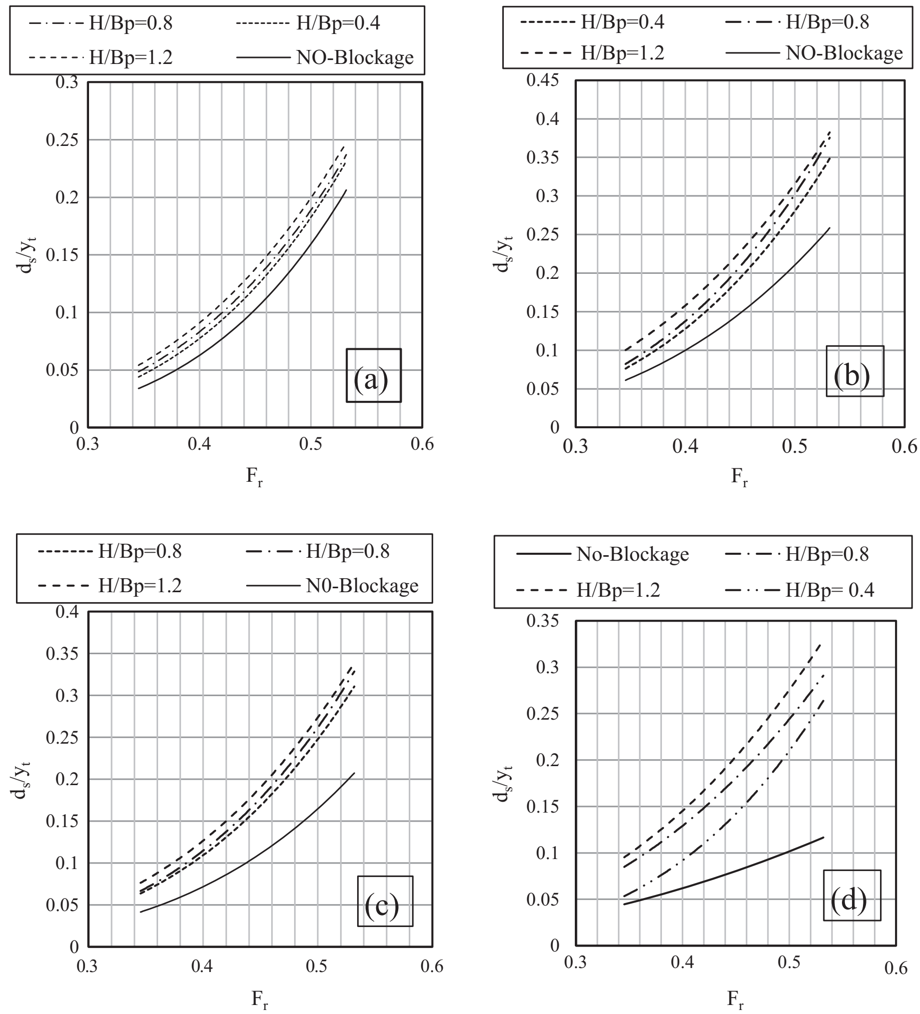

Figure 10 The relationship between d_s/y_t and F_r for $W/L = 2.2$ and different ratios of H/B_P for (a) left abutment and (b) left pier, (c) right abutment, and (d) upstream blockage at the right pier.

respectively. These figures show that the maximum relative scour depth (d_s/y_t) increases as the tail Froude number (F_r) increases. In addition, the relative scour depth (d_s/y_t) increases by increasing the relative width of blockage (W/L). The impermeable blockage in front of Pr increases the local scour depth at left pier (P_L) by 2.6%, 10.5%, 18.5%, 21%, 65%, and 86% while the local scour depth at Ar was increased by 7.4%, 28.7%, 41%, 50%, 64.7%, and 135% for the ratio of $W/L = 0.7$, 1.0, 1.4, 2.2, 4.0, and 8.75 respectively. The theoretical results of local scour depth created by the 3-D computational fluid dynamic model were compared to the measured data as presented in Fig. 7. The correlation coefficient between observed and simulated values was 0.86. The scour iso contour lines for the no-blockage and other blockage cases are shown in Fig. 8. The local scour depth generated at left pier is high compared to the other bridge supports. In addition, as the relative width of partial blockage increases the scour hole dimension for the two adjacent bridge supports increases, i.e. Ar and P_L. Horizontal velocity distribution at distance from bed equals $0.03y_t$ for different ratios of W/L are shown in Fig. 9. The velocities at the P_L are larger for $W/L = 8.75$ compared to the other relative widths of partial blockage. So, the high velocity concentration produces stronger horseshoe vortex causing higher local scour depth upstream of the left pier. It was found from these figures, that velocity concentration at the outer parts of the partial blockage increases as the ratio of W/L increases, leading to larger values of local scour depths around the right abutment and left pier of bridge.

5.2. Effect of different ratios of (H/Bp) on local scour depth

The effect of different relative heights of impermeable obstruction ($H/B_p = 0.4$, 0.8, and 1.2), at front of the Pr on local scour depth at multi-vents bridge supports, was investigated. The relationship between d_s/y_t and F_r at $W/L = 2.2$ is shown in Fig. 10. The local scour depth increases as the relative height of obstruction and Froude number increases. The increase in the obstacle height increases the area that objected to flow direction, and redistribution of velocity around the obstacle is generated to have more scour hole dimensions at Ar and P_L. The scour contour maps for different relative heights of partial blockage are shown in Fig. 11. It was found that, the scour hole dimension for relative height $H/B_p = 0.4$ is smaller

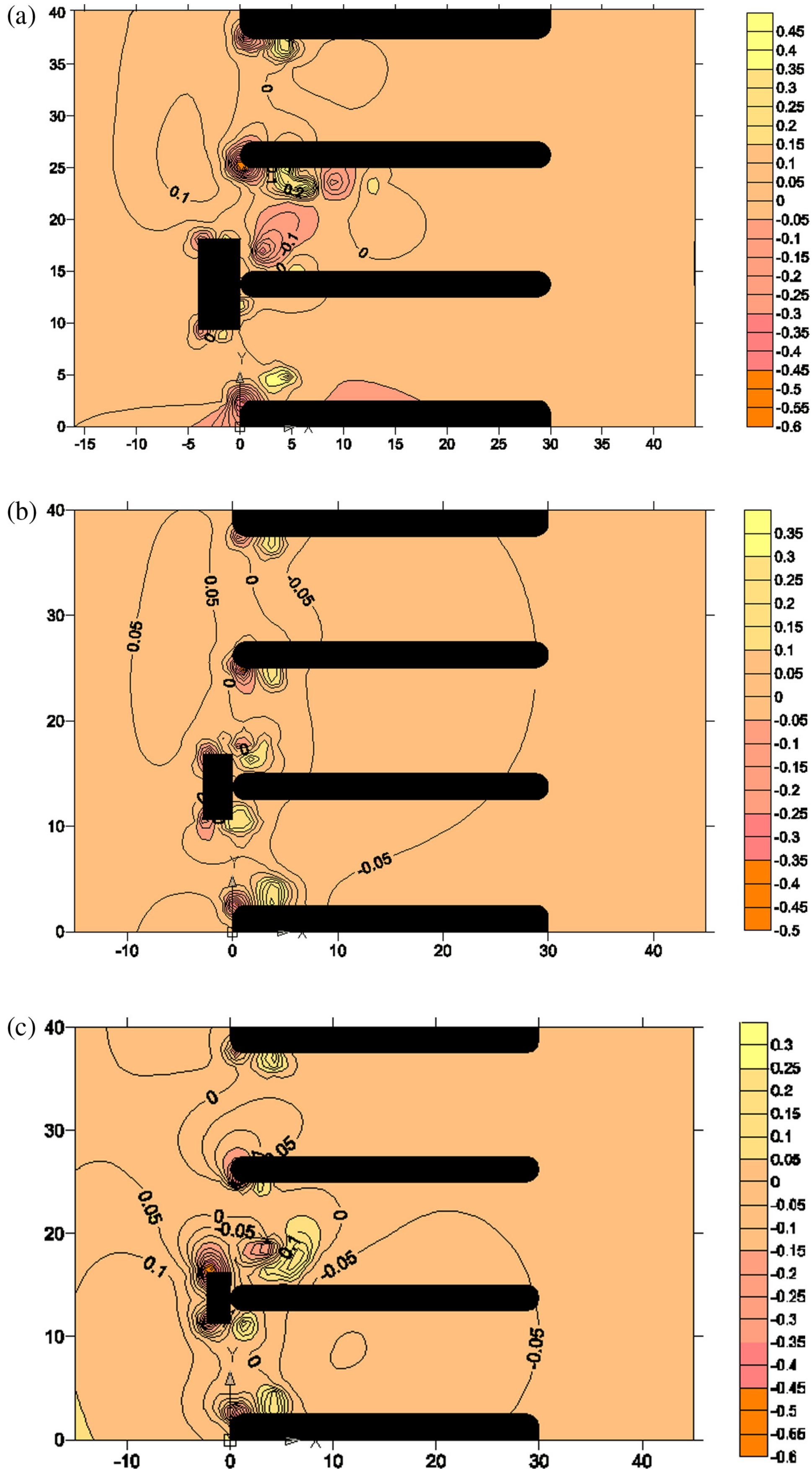

Figure 11 Scour contour maps for (a) $H/B_P = 0.4$, (b) $H/B_P = 0.8$ and (c) $H/B_P = 1.2$ at $W/L = 2.2$ and $F_r = 0.42$.

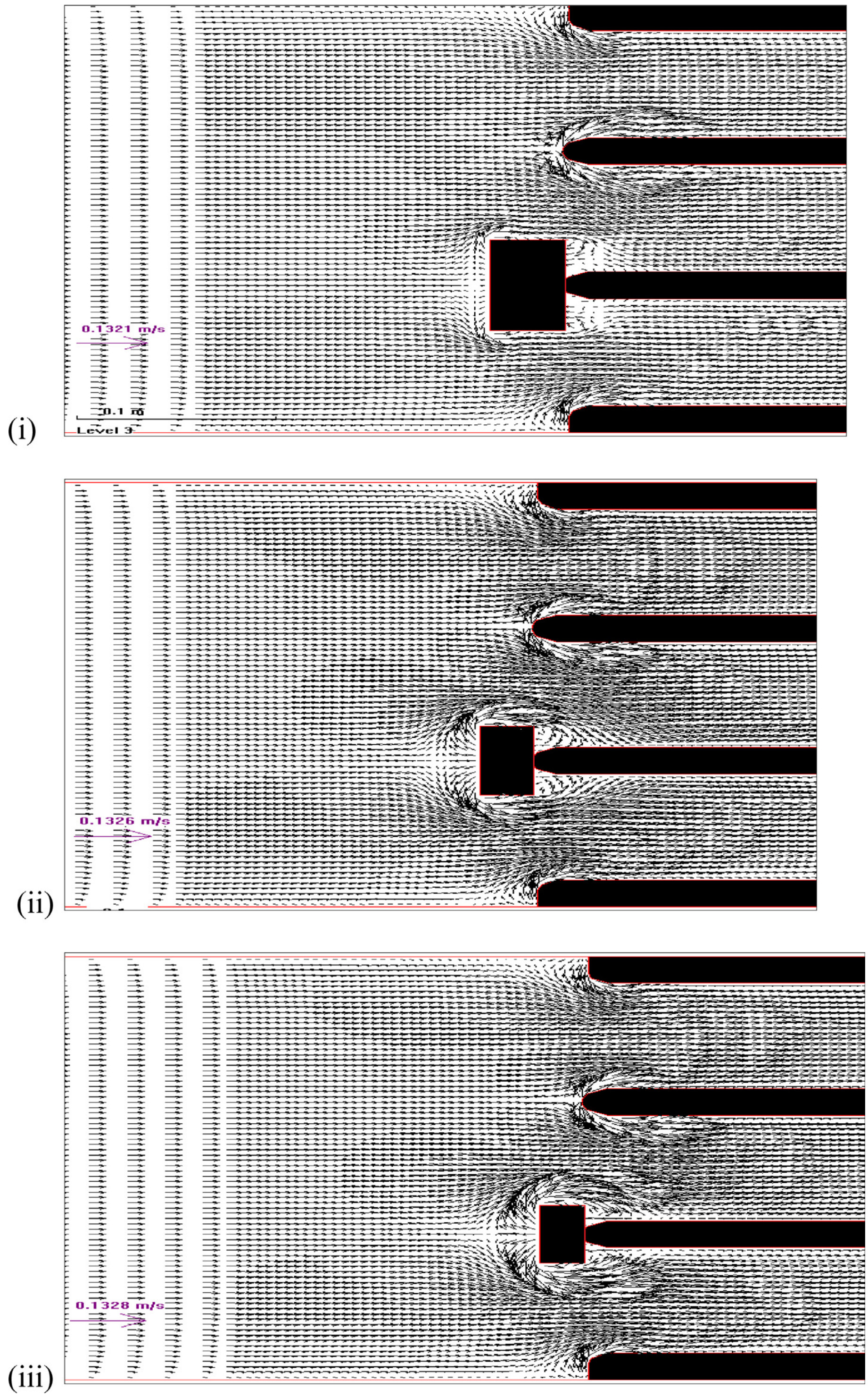

Figure 12 Velocity distribution for Plan cross section at 0.03 y_u for (i) H/B_P = 0.4, (ii) H/B_p = 0.8, and (iii) H/B_P = 1.2 at W/L = 2.2 and F_r = 0.42.

compared to the other ratios of H/B_p = 0.8 and 1.2. The maximum relative scour depth for different ratios of H/Bp (0.4, 0.8 and 1.2) increased by 34%, 47%, and 60% and 50%, 62%, and 73% for P_L and Ar, respectively at W/L = 2.2. Figs. 12 and 13 present the horizontal velocity vectors for different ratios of H/B_p. It is noticeable that the velocity vectors surrounding the obstruction increase as the relative height of partial blockage increases. The measured and simulated bed level using the computational fluid dynamic model for the different ratios of H/B_p is presented in Fig. 13. These figures show that, the results of 3-D computational fluid dynamic model agree well with measured data.

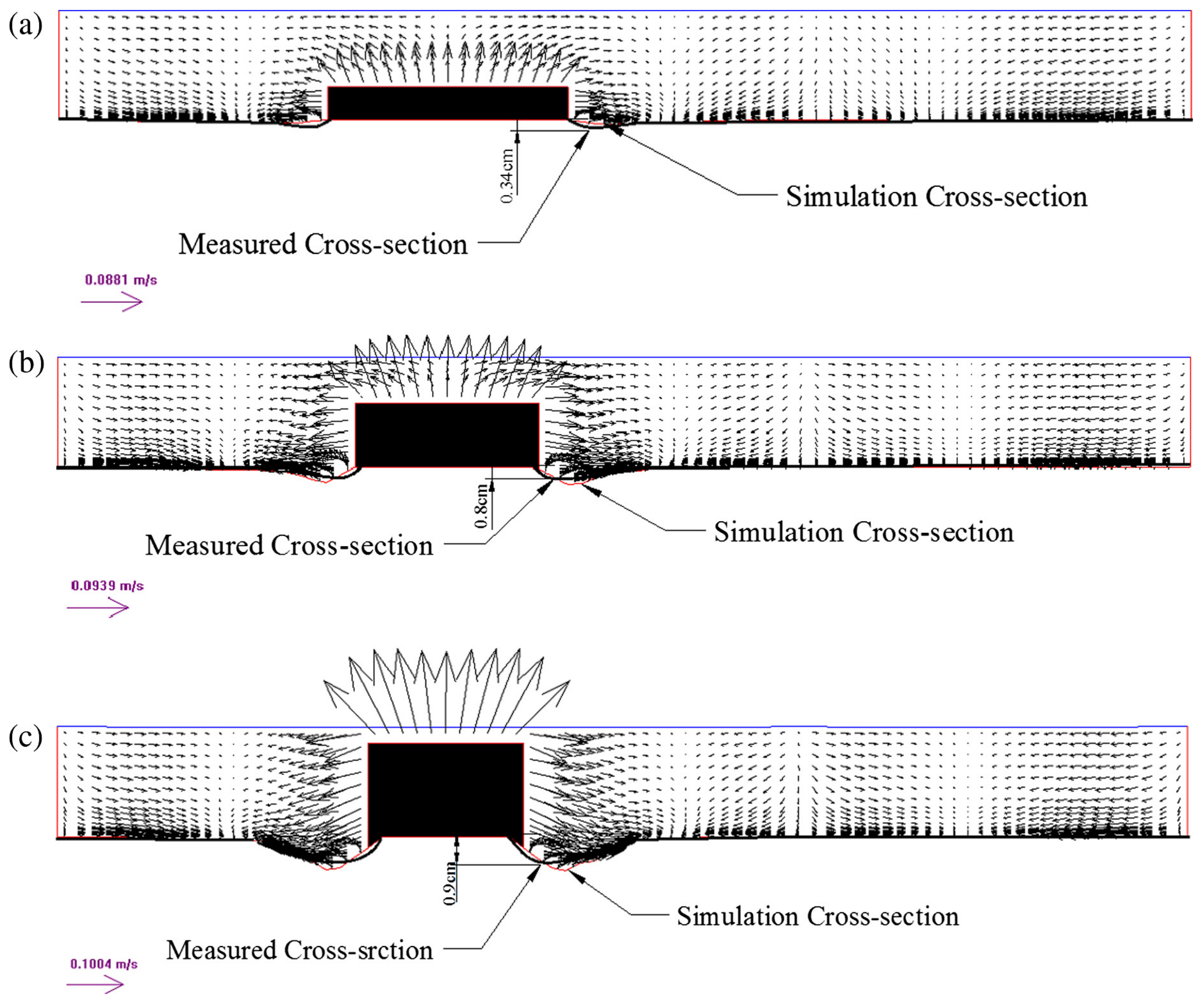

Figure 13 Velocity distribution for Lateral cross section for (a) $H/B_P = 0.4$, (b) $H/B_P = 0.8$ and (c) $H/B_p = 1.2$ at $W/L = 2.2$ and $F_r = 0.42$.

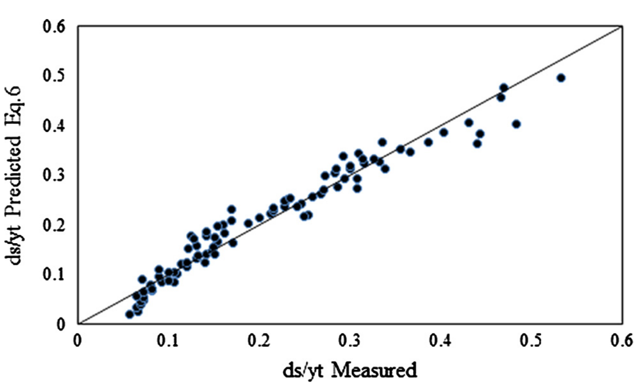

Figure 14 Predicted values of Eq. (6) versus measured data for relative scour depth d_s/y_t at left pier (P_L).

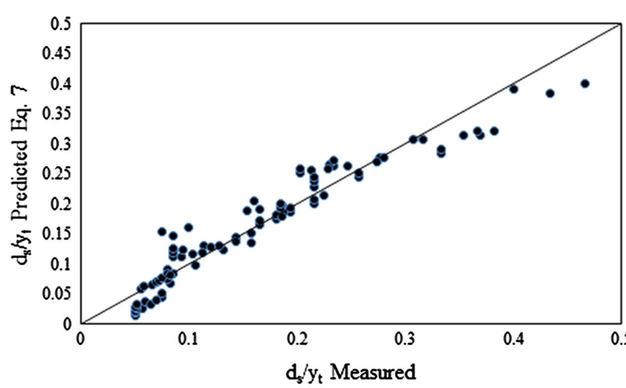

Figure 15 Predicted values of Eq. (7) versus measured data for relative scour depth d_s/y_t at the right abutment (Ar).

6. Regression models

Multiple linear regression analysis was used to correlate the relative local scour depth with other independent parameters. The proposed equations were used to compute the maximum local scour depth a result of partial blockage at Pr. These equations were developed for the left pier and right abutment at which lager values of local scour depth were obtained compared to the other supports. The correlation coefficients and standard errors of Eq. (6), which predict the maximum local sour depth at P_L, are 95% and 0.027, respectively. Eq. (7) has correlation coefficient and standard error of 92.3%, and

0.028, respectively at Ar. The measured data are compared to the predicted data for P_L and Ar. It was found that the proposed equations express well the measured data as shown in Figs. 14 and 15.

$$d_s/y_{t(P_L)} = -0.53 + 0.020(W/L) + 1.50(F_r) + 0.049(H/Bp) \quad (6)$$

$$d_s/y_{t(Ar)} = -0.45 + 0.017(W/L) + 1.28(F_r) + 0.018(H/Bp) \quad (7)$$

7. Conclusions

Partial blockage in front of bridge pier has significant interest due to its influence on stream flow and scour formed around neighboring bridge supports. Experimental and numerical studies are carried out to clarify the effect of such obstructions on scour formed around bridge piers and abutments. It was found that, obstruction at front of the right pier resulted in increasing the local scour depth at left pier and right abutment by 86% and 135%, respectively compared to the No-blockage case. In addition, the 3-D computational fluid dynamic and regression models agree well with the experimental results.

References

[1] Franzetti S, Radice A, Rabitti M, Rossi G. Hydraulic design and preliminary performance evaluation of countermeasure against debris accumulation and resulting local pier scour on River Po in Italy. J Hydraulic Eng 2011;137(5):615–20.
[2] Douglas FS, Smith RH. Effects of large woody debris removal on physical characteristics of a sand-bed river. Aquatic Conserv: Mar Freshwater Ecosyst 1992;2:145–63.
[3] Bovis MJ, Jakob M. The role of debris supply conditions in predicting debris flow activity. Earth Surf Proc Land 1999;24:1039–54.
[4] Pagliara S, Carnacia I. Influence of large woody debris on sediment scour at bridge piers. Int J Sedim Res 2011;26:121–36.
[5] Douglas Jr Shields, Morin N, Cooper CM. Large woody debris structures for sand-bed channels. J Hydraulic Eng 2004;130 (3):208–17.
[6] Lee KT, Ho Y, Chyan Y. Bridge blockage and overbank flow simulations using HEC–RAS in the Keelung River during the 2001 Nari Typhoon. J Hydraulic Eng 2006;132(3):319–23.
[7] Zevenbergen LW, Lagasse PF, Clopper PE. Effects of debris on bridge pier scour. In: World environmental and water resources congress. p. 10.
[8] Hodi SB. Effect of blockage and densimetric Froude number on circular bridge pier local scour MSc Thesis. University of Windsor; 2009. p. 97.
[9] Reynaud DA. Effects of debris on bridge pier scour. National Academy of Sciences; 2010. p. 177.
[10] Schmocker L, Hager WH. Probability of drift blockage at bridge decks. J Hydraulic Eng 2010;137(4):470–9.
[11] D'Alessandro C. Effect of blockage on cylindrical bridge pier local scour Electronic Theses and Dissertations. Canada: University of Windso; 2013, Paper 4966.
[12] Tejada S. Effects of blockage and relative coarseness on clear water bridge pier scour. Electronic Theses and Dissertations. Paper 5055; 2013. p. 155.
[13] Maatooq JS. Interference of scouring action between pier and abutment. J Eng Tech 2007;26:52008.
[14] Nasr-Allah T Hemdan, Mohamed Y Abdallah, Abdel-Aal G Mohamed, Basiouny M, Abd-Elhasseb A. Experimental study on the effect of permeable blockage at front of one pier on scour depth at mult-vents bridge supports. JES, Assiut University, Faculty of Engineering 2015;43(3):311–29.
[15] Sanoussi AA, Habib EA. Local scour at rounded and sloped face piers with skew angles. ICCBT 2008 - D - (41); 2008. p. 439–62.
[16] Khwairakpam P, Ray SS, Das S, Das R, Mazumdar A. Scour hole characteristics around a vertical pier under clearwater scour conditions. ARPN J Eng Appl Sci 2012;7(6):649–54. Asian Research Publishing Network (ARPN).
[17] Mohamed YA, Abdel-Aal GM, Nasr-Allah TH, Awad AS. Experimental and theoretical investigations of scour at bridge abutment. J King Saud Univ Eng Sci 2013. http://dx.doi.org/10.1016/j.jksues.2013.09.005.
[18] Mohamed YA, Abdel-Aal GM, Nasr-Allah TH, Awad AS. Investigating the effect of curved shape of bridge abutment provided with collar on local scour, experimentally and numerically. Ain Shams Eng J 2015;6(2):403–11.
[19] Nohani E, Heidarnejad M. Experimental investigation of the effect of flow angle of attack on the rate of scour around the slotted bridge pier at different levels of river bend. Int J Res Appl Sci Eng Technol (IJRASET) 2014;2(XII):276–82.
[20] Akib S, Jahangirzadeh A, Bass H. Local scour around complex pier groups and combined piles at semi-integral bridge. J Hydrol Hydromech 2014;62(2):108–16.
[21] Mohammed YA, Saleh YK, Ali AM. Experimental investigation of local scour around multi-vents bridge piers. Alexandria Eng J 2015;54:197–203.
[22] Nasr-Allah T Hemdan, Mohamed Y Abdallah, Abdel-Aal G Mohamed, Awad AS. Experimental and numerical simulation of scour at bridge abutment provided with different arrangements of collars. AEJ 2016;55(2):1455–63.
[23] Van Rijn LC. Mathematical modeling of morphological processes in the case of suspended sediment transport Ph.D. Thesis. Delft University; 1987.

Mr. Yasser A.M. Moussa received the M.Sc. and Ph.D. degrees in Civil Engineering Department from College of Engineering, Zagazig University, Egypt, in 2002 and 2005 respectively. During 2009, Dr Yasser Moussa was a Post Doctorate fellow with Hydroscience and Engineering, College of Engineering, University of Iowa, USA. Currently, he is an associate professor at college of engineering, Zagazig University, Egypt. His research interests are open channel hydraulics, stilling basins, sediment transport, simulation models, water resource managements, and artificial intelligence.

Mr. Tarek H. Nassralla received the M.Sc. degree in civil engineering department from Benha faculty of engineering, Benha University, Egypt, in 2001 and Ph.D. degree in civil engineering department from faculty of engineering, Minoufiya University, Egypt, in 2008. Currently, he is an Assistant Professor, Civil Eng Department, Benha University, Egypt. His research interests are open channel hydraulics, weeds, seepage, scour and irrigation development.

Eng. Amera Abdel Hasseb is Graduate student, Benha University, Faculty of Engineering.